

Single-Molecule SERS Spectroscopy

Katrin Kneipp^{1,2,3}, Harald Kneipp², and Henrik G. Bohr³

¹ Harvard-MIT Division of Health Sciences and Technology, Cambridge, MA 02139, USA

² Wellman Center for Photomedicine, Harvard University, Medical School, Boston, MA 02114, USA

³ Quantum Protein Center, Technical University of Denmark, DK-2800, Lyngby, Denmark
kneipp@usa.net

1 Introduction

It has long been the dream of chemists to examine a single molecule and monitor its structural changes. The observation of a single molecule and its individual properties and structural transformations can provide useful insight into the nature of processes that cannot be studied in an ensemble of molecules due to averaging. Moreover, high-throughput structurally selective detection of single molecules and quantification of matter by counting single molecules represent the ultimate limit in chemical analysis and trace detection. Today, single-molecule studies are a topic of rapidly growing scientific and practical interest in many fields, such as chemistry, physics, life sciences, and nanotechnology [1, 2, 3]. Photons have been identified as nearly perfect tools for detecting and studying single molecules. For example, the first single-molecule detection under ambient conditions was achieved using laser-induced fluorescence [4]. However, particularly under ambient conditions, there is a limited amount of molecular information that can be obtained from a fluorescence signal.

Raman spectroscopy as a vibrational technique provides a high degree of structural information but the extremely small cross section of the effect, typically $\sim 10^{-30} \text{ cm}^2$ to 10^{-25} cm^2 , with the larger values occurring only under favorable resonance Raman conditions, precludes the use of Raman spectroscopy as a method for single-molecule detection. For example, the number of Stokes photons can be estimated as the product of Raman cross section and excitation intensity: Assuming a Raman line with a scattering cross section of 10^{-29} cm^2 and 100 mW excitation light focused to $1 \mu\text{m}^2$, a single molecule scatters $\sim 10^{-4}$ photons per second, which means that one must wait more than an hour for a Stokes photon from a single molecule. In comparison, fluorescence cross sections are $\sim 10^{-16} \text{ cm}^2$.

Estimated enhancement factors for the Raman signals in SERS started from modest factors of 10^3 to 10^5 in the initial SERS experiments [5, 6]. For excitation laser wavelengths in resonance with the absorption band of the target molecule, surface-enhanced resonance Raman scattering (SERRS)

benefits from a superposition of surface enhancement and resonance Raman effect and can result in higher total effective Raman cross sections. Enhancement factors on the order of about 10^{10} to 10^{11} for rhodamine 6G and other dyes adsorbed on colloidal silver and excited under molecular resonance conditions have been reported by several authors in independent experiments [7, 8, 9, 10, 11, 12, 13, 14], based on a comparison of SERRS signals with fluorescence or with normal Raman signals of nonenhanced molecules such as methanol. In 1988, we measured SERRS spectra from about 100 rhodamine 6G molecules in a solution of small silver aggregates and concluded that in principle, even lower detection limits in SERS may be possible than were obtained with fluorescence [12, 15]. These results were confirmed in 1995 when we collected SERRS signals from 60 rhodamine 6G molecules and found that single-molecule Raman spectroscopy could be possible by further improving the experimental conditions [16].

However, SERS enhancement factors were underestimated in all these experiments for many years as they were inferred from a comparison between surface-enhanced Raman signals and normal Raman scattering or fluorescence. The main reason for this underestimation is that we do not know how many molecules are involved in the SERS process. The applied assumption that all molecules in a SERS experiment contribute to the observed SERS signal always results in estimating too small enhancement factors. In order to avoid this problem, we invented a different approach in which both surface-enhanced Stokes *and* anti-Stokes Raman scattering were used to extract information on the effective SERS cross section [17]. The idea behind this experiment was that a very strong Raman process can measurably populate the first vibrational level in addition to the thermal population. The effective Raman cross section, operative in this vibrational pumping process, can be inferred from the deviation of the anti-Stokes to Stokes signal ratio from the expected Boltzmann population. We discuss this effect in more detail in another Chapter in this book. Using this approach, we inferred effective SERS cross sections in nonresonant experiments that exceeded all previous assumptions and result in SERS enhancement factors of at least 10^{14} , amounting to nearly ten orders of magnitude higher than assumed in the first SERS experiments, but also at least 2 to 3 orders of magnitude higher than concluded from former SERRS studies. Effective SERS cross sections inferred from vibrational pumping were on the same order of magnitude as good fluorescence cross sections, making SERS spectroscopy of single molecules a realistic goal.

Two options have been used to achieve single-molecule sensitivity in a SERS experiment. One is based on the extremely large SERS enhancement factors obtained on silver and gold colloidal clusters at near-infrared excitation [18, 19, 20]. No resonance Raman effect for the target molecule is required in these experiments. A second approach exploits a favorable superposition of surface enhancement and resonance Raman enhancement of the analyte molecule, and is performed using excitation wavelengths within or close to the absorption band of the analyte molecule [21, 22, 23].

In this Chapter we will focus on single-molecule surface-enhanced Raman scattering experiments using near-infrared excitation where no resonance Raman effect contributes to the observed total enhancement. This is particularly true for adenine, which absorbs in the UV at 270 nm and is excited at 830 nm. Two types of SERS-active nanostructures will be used, colloidal nanoclusters in solution and fractal cluster structures on surfaces. These experiments will confirm many of the theoretical results discussed in the previous chapters, but will also show that there are still unanswered questions related to single-molecule Raman spectroscopy. In Sect. 3, we will consider some aspects of SERS as a single-molecule tool, and compare it with single-molecule fluorescence.

2 Single-Molecule SERS Experiments

Electromagnetic and chemical effects can account for the highest observed SERS enhancement on the order of 10^{14} . Theoretical estimates show that in principle, two kinds of composites of nanoparticles can account for the hot spots providing giant electromagnetic SERS enhancement: 1. Dimers and small aggregates formed from silver and gold nanoparticles [24, 25, 26, 27], where strong field enhancement exists particularly at the intersection between two nanoparticles, and 2. fractal types of nanostructures, which are comprised of aggregates and clusters formed by the self-assembling of nanoparticles [28, 29, 30, 31].

Electromagnetic effects in fractal structures can result in enhancement factors up to 10^{12} and even higher. Recent studies show that combining plasmon resonances and photonic resonances can give rise to electromagnetic enhancement factors sufficient for single-molecule Raman detection without chemical enhancement [32]. The extent of electronic enhancement to single-molecule SERS remains a subject of discussion [22, 33, 34], but there is compelling evidence that single-molecule Raman spectroscopy is primarily a phenomenon associated with the enhanced local optical fields in the vicinity of metal nanostructures. The high local optical fields in the hot spots of silver and gold cluster structures can be considered the key effect in SERS at an extremely high enhancement level [18, 35, 36, 37, 38]. This is also supported by the scaling of the enhancement factors for SERS and SEHRS as we have discussed previously in another Chapter. Large effective SERS cross sections allow the detection of single molecules based on pumped anti-Stokes SERS spectra [19, 39].

Figure 1 shows gold nanoclusters in various size ranges providing a high enough enhancement level for single-molecule Raman experiments. Larger aggregates show a fractal nature [40, 41].

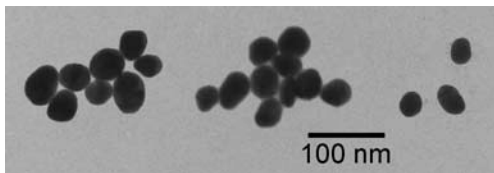


Fig. 1. Isolated gold nanoparticles and gold aggregates

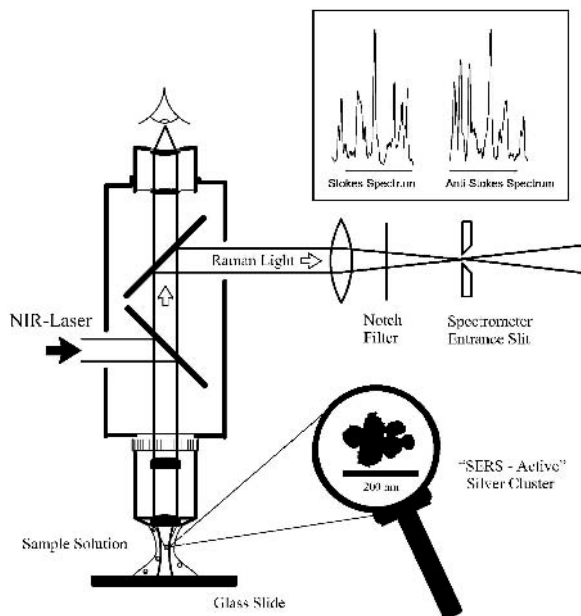


Fig. 2. Schematic of a typical single-molecule SERS experiment. Reprinted with permission from [37], Copyright 2002 Institute of Physics Publishing, Ltd

2.1 Single-Molecule SERS on Silver and Gold Nanoclusters in Solution

Figure 2 shows a schematic of a typical single-molecule SERS experiment performed in silver or gold colloidal solution [18, 19, 20]. Spectra are excited by a cw Ti:sapphire laser operating at 830 nm. A microscope attachment is used for laser excitation and collection of the Raman scattered light. The analyte is added to the solution of small silver or gold colloidal clusters (for example, see Fig. 1).

Concentration ratios of nanoclusters and target molecules of at least 10 make it unlikely that more than one analyte molecule will attach to the same colloidal cluster, avoiding formation of aggregates of the target molecules on the surface. Application of the analyte at such low concentration does not induce coagulation of the colloidal particles/colloidal clusters, and avoids for-

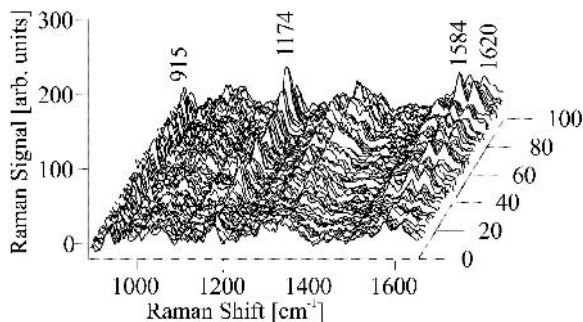


Fig. 3. 100 single-molecule SERS spectra of crystal violet on silver colloidal clusters. Collection time was one second for one spectrum, 830 nm excitation. Reprinted with permission from [18], Copyright 1997 American Physical Society

mation of larger clusters. The described procedure results in individual single molecules that are adsorbed on silver colloidal clusters. Analyte concentrations on the order of 10^{-12} M to 10^{-14} M and probed volumes whose sizes are on the order of femtolitre to picolitre result in average numbers of one or fewer target molecules in the focus volume.

The Brownian motion of single analyte molecule-loaded silver or gold clusters into and out of the probed volume results in strong statistical changes in the height of Raman signals measured from such a sample in time sequence. This is demonstrated in Fig. 3 that shows typical unprocessed SERS spectra measured in a time sequence from a sample with an average of 0.6 crystal violet molecules in the probed 30 pl volume [18]. Figure 4 displays the peak heights of the 1174 cm^{-1} crystal violet Raman line for the 100 SERS spectra (top), the background level of the colloidal solution with no analyte present (middle), and 100 measurements of the 1030 cm^{-1} Raman line of 3 M methanol in colloidal silver solution with about 10^{14} molecules of methanol in the scattering volume (bottom).

The SERS signals appear at different power intervals, which can be assigned “0”-, “1”-, “2”-, and “3”-molecule events. The normal Raman signal of the 10^{14} methanol molecules appears at about the same level as the SERS signal of a single-crystal violet molecule, confirming an enhancement factor on the order of 10^{14} . The inserts in Fig. 4 show the statistical distribution of the Raman and SERS signals. As expected, the methanol Raman signals collected in time sequence displays a Gaussian distribution. In contrast, the statistical distribution of the “0.6-molecules SERS signal” exhibits four relative maxima that are reasonably fit by the superposition of four Gaussian curves. The gradation of the areas of the four statistical peaks are roughly consistent with a Poisson distribution for an average number of 0.5 molecules. This reflects the probability of finding 0, 1, 2 or 3 molecules in the scattering volume during the actual measurement. Comparing the measured Poisson distribution with the 0.6-molecule concentration/volume estimate,

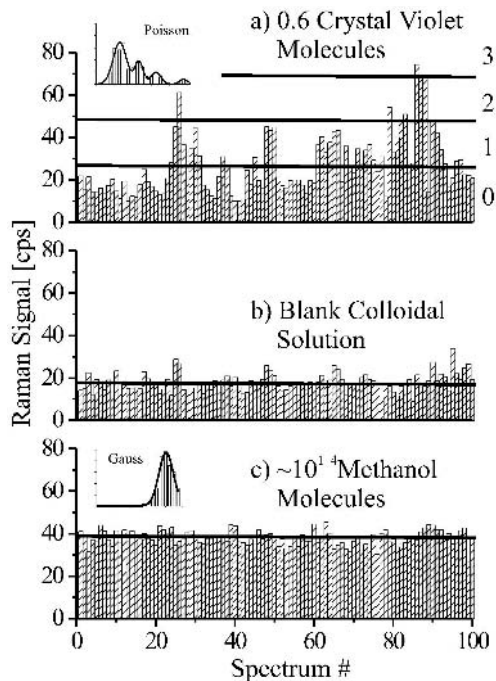


Fig. 4. Peak heights of the 1174 cm^{-1} SERS line from an average of 0.6 crystal violet molecules (*top*), background signal of a Raman line measured from 10^{14} methanol molecules (*below*). The *horizontal lines* display the thresholds for one-, two- and three-molecule signals (*top*), the average background (*middle*), and the average 10^{14} -molecule signal (*below*). The *inserts* show the Poisson and Gaussian statistics of single-molecule and many-molecule Raman signals, respectively. Reprinted with permission from [18], Copyright 1997 American Physical Society

we conclude that about 80% of molecules are detected by SERS. This statistical behavior of single-molecule SERS signals has been corroborated in several other studies [19, 20, 42]. The change in the statistical distribution of the Raman signal from Gaussian to Poisson when the average number of target molecules in the scattering volume is one or less is evidence for single-molecule detection by SERS. Fluctuations in the SERS signal of the target molecule are described by the Poisson statistics, and therefore reflect only Brownian motion of the silver or gold nanoclusters.

A look at Fig. 3 also shows fluctuations and changes in the SERS spectra collected in time sequence. Sometimes, new Raman lines appear in a spectrum, which do not exist in the following trace. The “new” spectral features do not correlate with the spectral signal strengths of the target molecule. We ascribe these Raman lines to the surface-enhanced spectra of impurities at the surface of the colloidal particles, which are probably introduced in the chemical preparation process. The impurity spectra change due to different colloidal clusters, which move into the focal volume loaded with different impurities.

The SERS signal of a target molecule at an extremely low concentration can vanish in a background SERS signal of impurities on the colloidal particles. This observation was discussed in our first studies of SERS spectroscopy

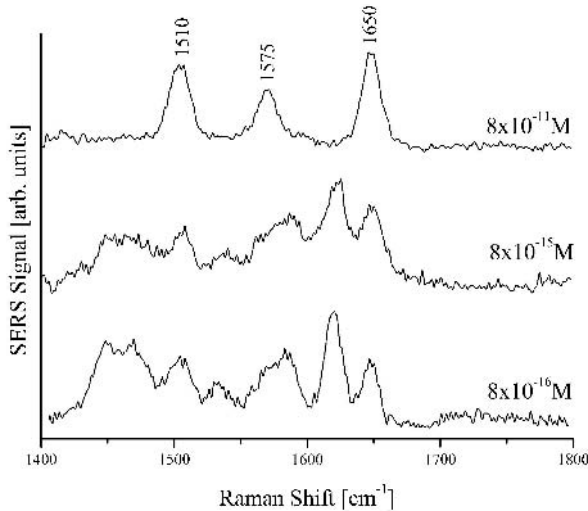


Fig. 5. SERS spectra of rhodamine 6G in silver colloidal solution in concentrations between 10^{-11} M and 10^{-16} M along with SERS spectra of impurities

at the single-molecule level [12, 16]. Figure 5 demonstrates this effect for the SERS spectrum of rhodamine 6G in a silver colloidal solution.

2.2 Single-Molecule SERS on Fixed Fractal Silver and Gold Cluster Structures

As discussed above, areas of particularly high local optical fields can also exist on silver and gold fractal structures formed, for example, by aggregation of colloidal particles of these metals. Near-field images taken on top of silver-cluster structures confirm the existence of optical hot spots and “cold zones” [43]. The dimensions of these hot spots can be orders of magnitude smaller than the wavelengths of light [44]. Since SERS takes place in the local fields of metallic nanostructures, the probed volume is determined by the confinement of the local fields, which can be two orders of magnitude smaller than the diffraction limit. The strongly confined hot spots provide the opportunity to spectroscopically select single nano-objects or molecules within a larger population. This was demonstrated in SERS experiments performed on bundles of single-wall carbon nanotubes (SWNTs) on fractal silver cluster structures [45, 46]. Usually a bundle of nanotubes gives rise to inhomogeneously broadened Raman lines due to tubes of different diameters present in the bundle. By scanning over nanotube bundles in contact with a fractal silver surface, one can sometimes measure SWNT spectra showing a very narrow linewidth without the sign of inhomogeneous broadening, indicating that this spectrum must originate from a single SWNT, or at most, from

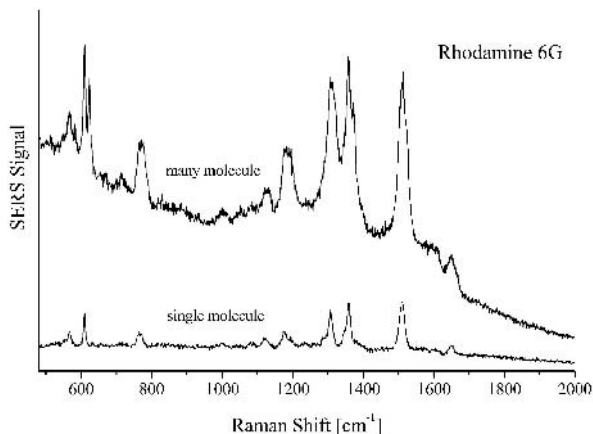


Fig. 6. Many-molecule (*top*) and single-molecule (*bottom*) SERS spectra of rhodamine 6G measured at different places on a fractal silver surface

very few tubes. The spectroscopic selection of single SWNTs within a bundle shows that SERS signals are collected from dimensions smaller than 5 nm.

It is interesting to compare SERS on the hot spots of nanoclusters with SERS exploiting local optical fields of metal tips [47, 48, 49]. In spite of the high field confinement for these tips, enhancement factors are reported to be orders of magnitude below those required for nonresonant single-molecule Raman spectroscopy. However, tip-enhanced Raman spectroscopy might approach the single-molecule level in combination with a very strong resonance Raman effect. For example, the technique can be used for studying single SWNTs because these tubes show an extremely strong resonance Raman effect based on resonances of the excitation and/or scattered photons with the van Hove singularities in the electronic energy levels of these one-dimensional carbon structures [50, 51].

The strong confinement of local optical fields is also demonstrated in Fig. 6, which shows two typical SERS spectra collected with a $\sim 1\ \mu\text{m}$ laser spot size from two different places at a fractal silver structure with an average of about 100 rhodamine 6G molecules in the $1\ \mu\text{m}$ spot. The upper spectrum reveals a many-molecule spectrum showing typical inhomogeneous broadening of the Raman lines due to the different environment of the rhodamine 6G molecules contributing to the spectrum on the silver surface. The bottom spectrum in Fig. 6 shows the Raman signal of a single rhodamine 6G molecule measured in a situation where a hot spot in the probed focal area selects a single molecule from a larger population of rhodamine 6G molecules present in the $1\ \mu\text{m}$ spot [52]. The single-molecule spectrum shows a clear decrease in linewidth compared to many-molecule SERS spectra as well as other changes due to different adsorption forms [53].

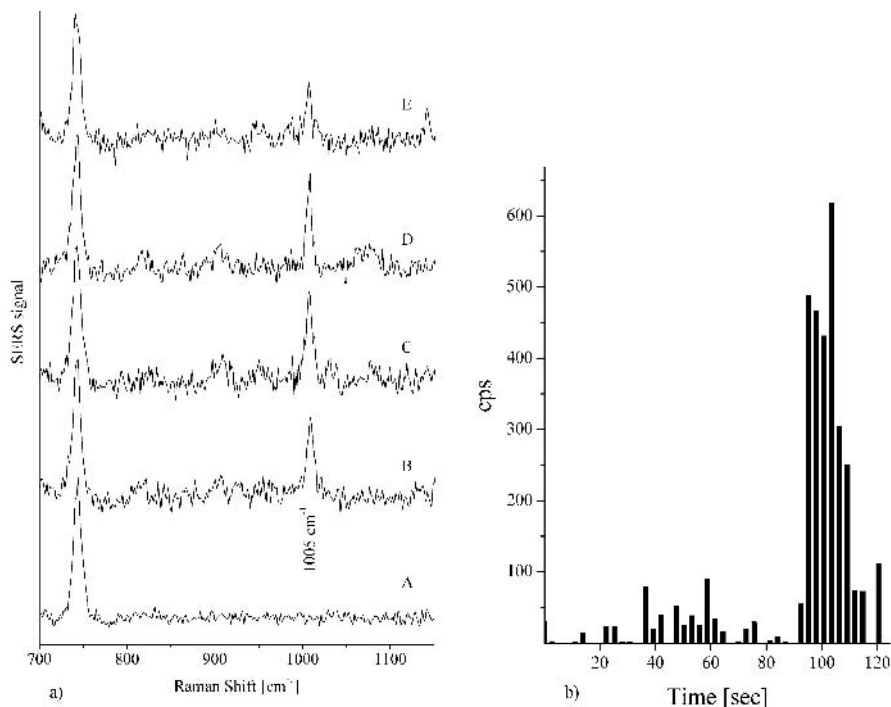


Fig. 7. (a) Selected single-molecule SERS spectra of enkephalin from one fixed spot on a fractal silver surface showing the 1000 cm^{-1} SERS line of phenylalanine and a line at 750 cm^{-1} , which can be ascribed to citrate on the silver colloids. (b) Time series of the 1000 cm^{-1} phenylalanine signal measured from one fixed spot on a sample with an average of one enkephalin molecule in the laser spot. Spectra were observed over a time interval of 120 s, 1 s collection time each. The signal level of 100 cps represents approximately the background level. Reprinted with permission from [54], Copyright 2004 IOS Press

We demonstrate the capability of fractal silver surfaces for single-molecule detection in Fig. 7, using the small protein enkephalin as a target molecule [54]. Enkephalin is a mixture of two pentapeptides, [Leu]enkephalin and [Met]enkephalin. Here we detect enkephalin at the single-molecule level based on the strongly enhanced ring-breathing mode of phenylalanine ($\sim 1000\text{ cm}^{-1}$), which is a building block of both pentapeptides. Figure 7a shows selected single-molecule SERS spectra measured in a time interval in a spectral window, which displays the 1000 cm^{-1} SERS line of phenylalanine and a line at about 750 cm^{-1} , which can be ascribed to a citrate impurity on the silver colloids. Figure 7b displays the Raman signal measured at 1000 cm^{-1} shift from the 830 nm excitation from the same $\sim 1\text{ }\mu\text{m}$ spot in a time sequence (1 s collection time each). Over the first 95 s, no SERS signal was measured. Then, a SERS signal appears relatively abruptly, stays for

about 20 s at the same level, and vanishes again. Such behavior, namely, the appearance of the 1000 cm^{-1} SERS signal within a 10 s to 30 s time window, has been observed in many measurements on single enkephalin molecules. If the enkephalin signal appears, it always appears at the same level. Spectra 7aB) to 7aE) were measured in the time window between 95 s and 115 s, spectrum 7aA) shows a situation when the 1000 cm^{-1} SERS signal does not exceed the noise level. A possible explanation for these changes in scattering power is that a single enkephalin molecule is diffusing on the colloidal silver cluster and can only be “seen” when it enters a hot spot.

Fluctuations in scattering power and/or sudden spectral shifts and changes that appear as a “blinking” of SERS signals have been reported by several authors [21, 23, 55]. Different effects can account for these spectral changes, such as thermally and nonthermally activated diffusion of molecules, as well as real transformations, such as protonation and deprotonation [56, 57]. Although blinking had been claimed as a hallmark of single-molecule detection, it has become evident that this behavior is not necessarily connected to single-molecule SERS. The effect has also been observed in lower-concentration “many-molecule” SERS spectra [58]. Fluctuations and changes in SERS spectra are discussed in more detail in several places in this book.

3 SERS as a Single-Molecule Analytical Tool – Comparison between SERS and Fluorescence

Ideally, one would like to have a spectroscopic tool that detects a single molecule and simultaneously identifies its chemical structure. A SERS spectrum, containing different vibrational modes, provides high structural information content on a molecule that is the equivalent of its fingerprint. At present, SERS is the only way to detect a single molecule and simultaneously identify its chemical structure. But, as we have demonstrated for enkephalin, also measuring only one typical SERS line of the target molecule and using this Raman line as an intrinsic spectroscopic signature for the specific molecule is a useful tool for detecting and tracking a known molecule without the use of a fluorescence tag.

If labeling of the target molecule should be necessary for any reason, SERS labels can provide several advantages compared to fluorescence tags. Under biologically relevant conditions, such as in solutions and at room temperature, fluorescence signals are very broad spectral signatures, typically 400 cm^{-1} to 800 cm^{-1} . Compared to a fluorescence band, SERS results in spectrally narrow lines typically 10 cm^{-1} to 20 cm^{-1} . Because of the high specificity of a Raman spectrum, spectral overlap between different labels is very unlikely, even when their molecular structures are very similar [36]. This results in a huge arsenal of potential SERS labels making possible multiplex detection [59]. Moreover, detecting a label based on a signature that

comprises several sharp lines allows for the application of spectral correlation techniques, and therefore improved contrast [60].

A principal advantage of SERS over fluorescence for single-molecule detection involves the total number of photons that can be emitted by a molecule. This is determined by the maximum number of excitation–emission cycles a molecule survives. In fluorescence experiments, this number is limited by the rate of photobleaching of the molecule. No photodecomposition has been observed in nonresonant SERS, and also in SERRS experiment the effect of bleaching is strongly reduced.

Another number that is of particular interest for the rapid detection and screening of single molecules is the maximum number of photons that can be emitted by a molecule per unit time. Under saturation conditions, this number is inversely proportional to the lifetime of the excited molecular states involved in the optical detection process. Due to the shorter vibrational relaxation times compared to the electronic relaxation times, a molecule can go through more Raman cycles than fluorescence cycles per time interval. Therefore, the number of Raman photons per unit time that can be emitted by a molecule under saturation conditions can be higher than the number of fluorescence photons by a factor of 10^2 to 10^3 [12].

In single-molecule SERS experiments in solution, the target molecule has to be attached to SERS-active nanoclusters (compare Sect. 2.1). This attachment of the target molecule to a much bigger particle can be an advantage for single-molecule detection as increased diffusion times minimize the possibility of the target molecule escaping out of the focal volume of the laser too rapidly.

For practical applications, it can be of interest to detect single molecules in a fluorescent environment. In this case, the background problem can be rigorously treated by using anti-Stokes SERS signals for single-molecule detection at the high-energy side of the excitation laser [19, 20].

3.1 Potential Applications of Single-Molecule Raman Spectroscopy

Single-molecule capabilities of SERS open up exciting perspectives and new aspects in the field of biophysics and biochemistry as compared to fluorescence, which is widely used as a single-molecule spectroscopic tool in this field [37]. For example, SERS opens up opportunities for monitoring proteins at the single-molecule level in their natural aqueous environment.

One of the most spectacular potential applications of single-molecule SERS is in the field of rapid DNA sequencing at the single-molecule level [61]. These applications range from the use of Raman spectroscopic characterization of specific DNA fragments down to structurally sensitive detection of single bases without the use of fluorescent or radioactive tags, based on the intrinsic surface-enhanced Raman scattering of the base [20]. Effective

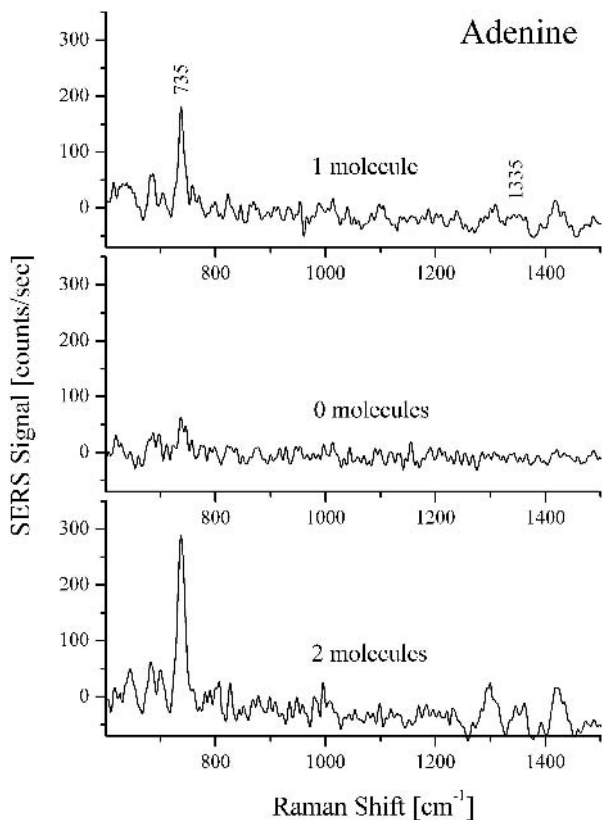


Fig. 8. SERS spectra of single adenine molecules in silver colloidal solution measured in one second collection time using 830 nm cw excitation. Reprinted with permission from [20], Copyright 1998 American Physical Society

SERS cross sections of the order of 10^{-16} cm² can be inferred for adenosine monophosphate (AMP) and for adenine on colloidal silver clusters. NIR-SERS spectra of adenine and adenosine monophosphate (AMP) are identical, indicating sugar and phosphate bonds do not interfere with the strong SERS effect of adenine.

Figure 8 displays situations in aqueous solution where “1”, “0”, or “2” adenine molecules attached to silver nanoclusters were present in the probed volume during the 1 s collection time. Due to the electromagnetic origin of the enhancement, it should be possible to achieve SERS cross sections for other bases in the same order of magnitude as adenine when they are attached to colloidal silver or gold clusters. The nucleotide bases show well-distinguished surface-enhanced Raman spectra, also shown in Fig. 9. Thus, after cleaving single native nucleotides from the DNA or RNA strand into a medium containing colloidal silver or gold clusters, direct detection and identification of

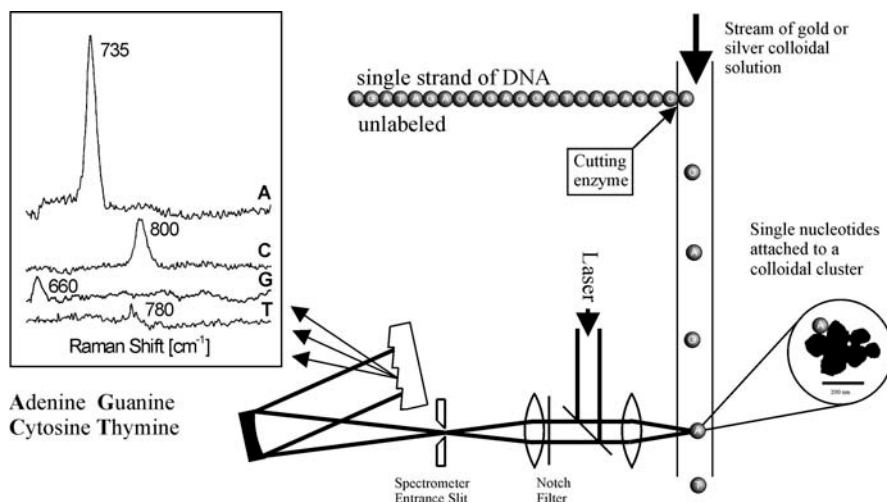


Fig. 9. Schematic of DNA sequencing based on the intrinsic Raman spectra of the four bases. Reprinted with permission from [37], Copyright 2002 Institute of Physics Publishing, Ltd

single native nucleotides should be possible, due to the unique SERS spectra of their bases. SERS active silver or gold nanoclusters can be provided in a flowing stream of colloidal solution or onto a moving surface with silver or gold cluster structures.

It is interesting to estimate the detection rate of single nucleotides in such an experiment. Single-molecule adenine spectra can be measured at good signal-to-noise ratios of 10 in a 1 s collection time at $3 \times 10^5 \text{ W/cm}^2$ excitation. Assuming a SERS cross section on the order of 10^{-17} to 10^{-16} cm^2 and a vibrational lifetime on the order of 10 ps, saturation of SERS will be achieved at 10^8 to 10^9 W/cm^2 excitation intensity. Extrapolation to saturation conditions shows that single-molecule SERS spectra over the complete fingerprint region (ca. 700 cm^{-1} to 1700 cm^{-1}) should be measurable in ms or at kHz rates.

4 Conclusion

Numerous experiments conducted during the last decade have demonstrated that SERS enables the measurement of Raman spectra of single molecules, one at a time. Presently, single-molecule experiments without the resonance Raman contribution of the target molecule require SERS enhancement factors of 10^{13} to 10^{14} . In principle, electromagnetic and/or chemical effects can account for this enhancement level. Theoretical estimates for different silver and gold nanostructures from dimers to self-similar structures show that local

optical fields in hot spots can give rise to SERS enhancement factors of up to 10^{12} and even higher. However, in many experiments, electronic effects might contribute in order to match the experimentally observed effective cross sections. The extent of electronic enhancement remains a subject of discussion. There is evidence that SERS is primarily a phenomenon associated with the enhanced local optical fields in the vicinity of metal nanostructures. Enhanced and strongly confined fields are always associated with high field gradients. These large field gradients may direct molecules to the hot spot and hold them there for detection.

As a single-molecule tool, SERS opens up some exciting potential capabilities as compared with fluorescence, another widely used single-molecule technique. To detect and identify single molecules by fluorescence, in many cases the molecules must be labeled to achieve large enough quantum yields and distinguishable spectral properties. However, in each case, the structural information on the target molecule is very limited, particularly under ambient conditions. SERS is a method for detecting *and* identifying a molecule without any labeling because it is based on the intrinsic Raman signature of the molecule. Moreover, Raman scattering is a very general property of a molecule, and almost every molecule has Raman-active molecular vibrations that can be “seen” by the Raman effect at a cross section of at least 10^{-30} cm², whereas far fewer molecules show fluorescence. For the detection of a molecule by SERS, it has to be attached to SERS-active substrates in order to increase its effective Raman cross section by 12–14 orders of magnitude. Due to the primarily electromagnetic origin of this enhancement, it should be possible to achieve an equally strong SERS effect for each molecule, thus making SERS a broadly applied tool for single-molecule detection.

Acknowledgements

This work is supported in part by DOD grant # AFOSR FA9550-04-1-0079 and by the generous gift of Dr. and Mrs. J.S. Chen to the optical diagnostics program of the Massachusetts General Hospital, Wellman Center for Photomedicine.

One of us (KK) would like to thank Michael S. Feld and Ramachandra R. Dasari for kind support and collaboration when performing the first single-molecule Raman experiments as Heisenberg Fellow at the G. R Harrison Spectroscopy Laboratory at MIT.

References

- [1] M. Eigen, R. Rigler: Proc. Nat. Acad. Sci. USA **91**, 5740 (1994)
- [2] X. S. Xie, J. K. Trautman: Ann. Rev. Phys. Chem. **49**, 441 (1998)
- [3] F. Kulzer, M. Orrit: Ann. Rev. Phys. Chem. **55**, 585 (2004)

- [4] R. A. Keller, W. P. Ambrose, P. M. Goodwin, et al.: *Appl. Spectrosc.* **50**, A12 (1996)
- [5] D. L. Jeanmaire, R. P. Van Duyne: *J. Electroanal. Chem.* **84**, 1 (1977)
- [6] M. G. Albrecht, J. A. Creighton: *J. Am. Chem. Soc.* **99**, 5215 (1977)
- [7] A. Bachackashvilli, S. Efrima, B. Katz, et al.: *Chem. Phys. Lett.* **94**, 571 (1983)
- [8] K. Kneipp, G. Hinzmann, D. Fassler: *Chem. Phys. Lett.* **99**, 5 (1983)
- [9] K. Kneipp, D. Fassler: *Chem. Phys. Lett.* **106**, 498 (1984)
- [10] P. Hildebrandt, M. Stockburger: *J. Phys. Chem.* **88**, 5935 (1984)
- [11] K. Kneipp, H. Kneipp, M. Rentsch: *J. Molec. Struct.* **156**, 3 (1987)
- [12] K. Kneipp: *Exp. Techn. Phys.* **36**, 161 (1988)
- [13] B. Pettinger, K. Krischer: *J. Electron. Spectrosc. Relat. Phenom.* **45**, 133 (1987)
- [14] B. Pettinger, K. Krischer, G. Ertl: *Chem. Phys. Lett.* **151**, 151 (1988)
- [15] D. C. Nguyen, R. A. Keller, M. Trkula: *J. Opt. Soc. Am. B: Opt. Phys.* **4**, 138 (1987)
- [16] K. Kneipp, Y. Wang, R. R. Dasari, et al.: *Appl. Spectrosc.* **49**, 780 (1995)
- [17] K. Kneipp, Y. Wang, H. Kneipp, et al.: *Phys. Rev. Lett.* **76**, 2444 (1996)
- [18] K. Kneipp, Y. Wang, H. Kneipp, et al.: *Phys. Rev. Lett.* **78**, 1667 (1997)
- [19] K. Kneipp, H. Kneipp, G. Deinum, et al.: *Appl. Spectrosc.* **52**, 175 (1998)
- [20] K. Kneipp, H. Kneipp, V. B. Kartha, et al.: *Phys. Rev. E* **57**, R6281 (1998)
- [21] S. Nie, S. R. Emory: *Science* **275**, 1102 (1997)
- [22] A. M. Michaels, M. Nirmal, L. E. Brus: *J. Am. Chem. Soc.* **121**, 9932 (1999)
- [23] H. X. Xu, E. J. Bjerneld, M. Kall, et al.: *Phys. Rev. Lett.* **83**, 4357 (1999)
- [24] H. Metiu: Possible causes for surface enhanced raman scattering, in W. F. Murphy (Ed.): *Proc. VIIth Int. Conf. Raman Spectrosc. Linear and Non Linear Processes* (North-Holland, Amsterdam 1980) pp. 382–384
- [25] M. Inoue, K. Ohtaka: *J. Phys. Soc.* **52**, 3853 (1983)
- [26] H. Xu, J. Aizpurua, M. Kaell, et al.: *Phys. Rev. E* **62**, 4318 (2000)
- [27] L. Gunnarsson, T. Rindzevicius, J. Prikulis, et al.: *J. Phys. Chem. B* **109**, 1079 (2005)
- [28] M. I. Stockman, V. M. Shalaev, M. Moskovits, et al.: *Phys. Rev. B* **46**, 2821 (1992)
- [29] E. Y. Poliakov, V. M. Shalaev, V. A. Markel, et al.: *Opt. Lett.* **21**, 1628 (1996)
- [30] Y. Yamaguchi, M. K. Weldon, M. D. Morris: *Appl. Spectrosc.* **53**, 127 (1999)
- [31] Z. J. Wang, S. L. Pan, T. D. Krauss, et al.: *Proc. Nat. Acad. Sci. USA* **100**, 8638 (2003)
- [32] S. L. Zou, G. C. Schatz: *Chem. Phys. Lett.* **403**, 62 (2005)
- [33] A. Otto: *J. Raman Spectrosc.* **36**, 497 (2005)
- [34] L. P. Capadona, J. Zheng, J. I. Gonzalez, et al.: *Phys. Rev. Lett.* **94**, 058301 (2005)
- [35] K. Kneipp, H. Kneipp, R. Manoharan, et al.: *Appl. Spectrosc.* **52**, 1493 (1998)
- [36] K. Kneipp, H. Kneipp, I. Itzkan, et al.: *Chem. Rev.* **99**, 2957 (1999)
- [37] K. Kneipp, H. Kneipp, I. Itzkan, et al.: *J. Phys.: Condens. Matter* **14**, R597 (2002)
- [38] M. Moskovits: *J. Raman Spectrosc.* **36**, 485 (2005)
- [39] K. Kneipp, H. Kneipp, I. Itzkan, et al.: *Chem. Phys.* **247**, 155 (1999)
- [40] D. A. Weitz, M. Oliveria: *Phys. Rev. Lett.* **52**, 1433 (1984)

- [41] K. Güldner, R. Liedtke, K. Kneipp, et al.: Morphological study of colloidal silver clusters employed in surface-enhanced Raman spectroscopy (SERS), in H. D. Kronfeldt (Ed.): *29th EGAS Berlin* (European Physical Society Berlin 1997) p. 128
- [42] P. Etchegoin, R. C. Maher, L. F. Cohen, et al.: Chem. Phys. Lett. **375**, 84 (2003)
- [43] P. Zhang, T. L. Haslett, C. Douketis, et al.: Phys. Rev. B **57**, 15513 (1998)
- [44] V. M. Shalaev: Phys. Rep. **272**, 61 (1996)
- [45] K. Kneipp, H. Kneipp, P. Corio, et al.: Phys. Rev. Lett. **84**, 3470 (2000)
- [46] K. Kneipp, H. Kneipp, I. Itzkan, et al.: Nonlinear Raman probe of single molecules attached to colloidal silver and gold clusters, in V. M. Shalaev (Ed.): *Optical Properties of Nanostructured Random Media* (Springer, Berlin, Heidelberg, New York 2002) pp. 227–247
- [47] N. Hayazawa, Y. Inouye, Z. Sekkat, et al.: Opt. Commun. **183**, 333 (2000)
- [48] A. Hartschuh, M. R. Beversluis, A. Bouhelier, et al.: Philos. Trans. Roy. Soc. London: A Math. Phys. Eng. Sci. **362**, 807 (2004)
- [49] B. Pettinger, B. Ren, G. Picardi, et al.: Phys. Rev. Lett. **92**, 096101 (2004)
- [50] M. S. Dresselhaus, G. Dresselhaus, A. Jorio, et al.: J. Nanosci. Nanotechnol. **3**, 19 (2003)
- [51] N. Anderson, A. Hartschuh, S. Cronin, et al.: J. Am. Chem. Soc. **127**, 2533 (2005)
- [52] K. Kneipp, H. Kneipp: Canadian J. Anal. Sci. Spectrosc. **48**, 125 (2003)
- [53] T. Vosgrone, A. J. Meixner: Chem. Phys. Chem. **6**, 154 (2005)
- [54] K. Kneipp, H. Kneipp, S. Abdali, et al.: Spectrosc. Int. J. **18**, 433 (2004)
- [55] M. Futamata, Y. Maruyama, M. Ishikawa: J. Molec. Struct. **735-36**, 75 (2005)
- [56] A. Weiss, G. Haran: J. Phys. Chem. B **105**, 12348 (2001)
- [57] Z. J. Wang, L. J. Rothberg: J. Phys. Chem. B **109**, 3387 (2005)
- [58] C. J. L. Constantino, T. Lemma, P. A. Antunes, et al.: Appl. Spectrosc. **57**, 649 (2003)
- [59] Y. C. Cao, R. C. Jin, J. M. Nam, et al.: J. Am. Chem. Soc. **125**, 14676 (2003)
- [60] J. Kneipp, H. Kneipp, W. L. Rice, et al.: Anal. Chem. **77**, 2381 (2005)
- [61] W. P. Ambrose, P. M. Goodwin, J. H. Jett, et al.: Berichte der Bunsen-Gesellschaft – Phys. Chem. Chem. Phys. **97**, 1535 (1993)

Index

- agents
 - adenine, 273
 - adenosine monophosphate, 272
 - enkephalin, 269
 - nucleotide bases, 272
 - pentapeptides, 269
 - rhodamine 6G, 262, 267
 - surface-enhanced, 263
- impurities, 266
- inhomogeneously broadened, 267
- methods
 - saturation conditions, 273
- multiplex detection, 270
- nanostructures
 - aggregates, 263, 269
- near-infrared excitation, 263
- plasmon
 - resonance, 263
- Raman scattering
 - anti-Stokes, 262
 - anti-Stokes SERS, 271
 - cross section, 262
 - SERS cross section, 262
- single molecule, 261, 264
 - detection, 269
 - experiments, 273
- single-wall carbon nanotubes, 267
- trace detection, 261
- vibrational pumping, 262
- vibrational relaxation times, 271
- DNA
 - sequencing, 271
- enhancement
 - chemical, 263, 274
 - electromagnetic, 263, 274
 - local field, 268
 - factor, 261
- fluctuations, 270
 - blinking, 270
 - Brownian motion, 265
 - diffusion times, 271
 - Gaussian distribution, 265
 - Poisson distribution, 265
 - statistical distribution, 266
- fluorescence, 274
 - cross section, 261
 - tag, 270
- hot spot, 267
- hyper-Raman scattering